



Dual-layer Gaussian process model for limit state analysis of natural rubber bridge isolators

Pedro A. C. Bandini^{1*}, Patrick Paultre²

¹Postdoctoral fellow, Department of Civil and Building Engineering, Université de Sherbrooke, Sherbrooke, Canada

²Professor, Department of Civil and Building Engineering, Université de Sherbrooke, Sherbrooke, Canada

*pedro.bandini@usherbrooke.ca (Corresponding Author)

ABSTRACT

A Gaussian process model composed of two layers (classification followed by regression) is constructed to estimate the limit state of natural rubber bridge isolators. Depending on the geometry and loading characteristics, natural rubber isolators can fail under buckling or shear. A dataset comprised of more than 8,000 numerical models is used for training and validation of the Gaussian process model. This dataset was previously built using a finite element model capable of simulating both the lateral deformation and the rupture type of rubber isolators. The first layer of the surrogate model separates the two types of limit state. The influence of the slenderness ratio and the axial loading is stressed in delineating the threshold between the two failure modes. Based on the geometric and loading properties within each limit state, a Gaussian process regression model estimates the distribution of critical shear strain of the elastomeric isolator. The outcomes of the dual-layer surrogate model can be used to build fragility curves for both specific isolation devices and entire populations, which are paramount for the seismic performance assessment of isolated bridges. Furthermore, the resulting model can be updated regarding the importance of the population of isolation devices found in practice.

Keywords: surrogate model, performance-based design, seismic isolator, buckling, shear.

INTRODUCTION

Seismic fragility analysis has demonstrated its efficiency in performance-based earthquake engineering (PBEE) for the last two decades. One essential step in the performance assessment is the definition of probabilistic capacity models (or fragility functions) of critical components of a structure [1-3]. Laminated natural rubber (NR) isolators installed in bridges is one of these components, which must sustain a combination of dead load and large lateral displacement during seismic excitation. In the case of exceptional ground shaking, NR isolators can be subjected to shear strains larger than 300%. In such extreme situations, these devices may fail either under buckling or tearing by shear failure [4]. It has been commonly accepted that the shape factor S (the ratio between the bounded and vertically loaded area and the free area of one rubber layer of the isolator) have an important role in the determination of the limit state (LS). Conversely, recent experimental and parametric studies have shown that the slenderness λ (the ratio of the total rubber height to the isolator width) has a more relevant influence on how the NR isolator might fail, while S has a limited impact. Moreover, a threshold $\lambda_{lim} = 0.4$ has been suggested to efficiently separate the two failure modes [4-6]. While slender isolators ($\lambda > \lambda_{lim}$) are subjected to instability by buckling, non-slender isolators ($\lambda < \lambda_{lim}$) are more likely to undergo tearing of a rubber layer by shear failure. Figure 1 schematically illustrates two isolators—one slender and one non-slender, both with a same shape factor—and their respective expected lateral responses and limit states. Bandini et al. [6] also addressed the influence of bearing loads on the shear strain capacity. The interaction between the geometric parameters and the bearing load, and the degree of uncertainty in the characterization of the limit states, however, have not been completely quantified. A statistical learning framework is leveraged to overcome the limitations of previous studies. More precisely, a dual-layer surrogate model based on Gaussian process (GP) is proposed to first establish the type of limit state to subsequently estimate the respective ultimate shear strain. The relevance of geometric and loading parameters are assessed throughout the surrogate modeling steps.

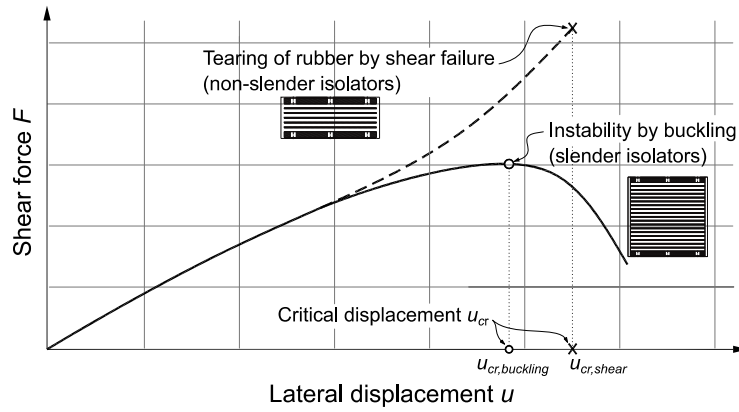


Figure 1: Limit states of natural rubber bridge isolators depending on the slenderness (adapted from Bandini et al. [6]).

DATASET ON LIMIT STATES OF NATURAL RUBBER ISOLATORS

In a recent parametric study, Bandini et al. [6] built a dataset with more than 8,000 numerical models of natural rubber square isolators. The numerical models were built upon a finite element (FE) model capable of simulating the lateral response of NR isolators and capturing the type of limit state [7]. The FE model was calibrated using laboratory data from a comprehensive experimental program [4]. The dataset contains the system parameters (shape factor S , slenderness ratio λ , and vertical loading P —Figure 2), the type of failure and the corresponding critical shear strain γ_{cr} (Figure 3). The dataset was built to cover the population of natural rubber bridge isolators commonly found in the literature involving research, design examples, and practice (e.g., [8-11]). All numerical models have, however, the same width $b = 900$ mm, which explains why this parameter was not included in the present study. Slenderness ratios and bearing loads are roughly uniformly distributed. For square bearings, shape factor and slenderness ratio are correlated through the number of rubber layers N_r ($\lambda S = N_r/4$), which explains the non-uniform distribution of the shape factor. Further details on the rationale to construct the dataset are found in Ref. [6].

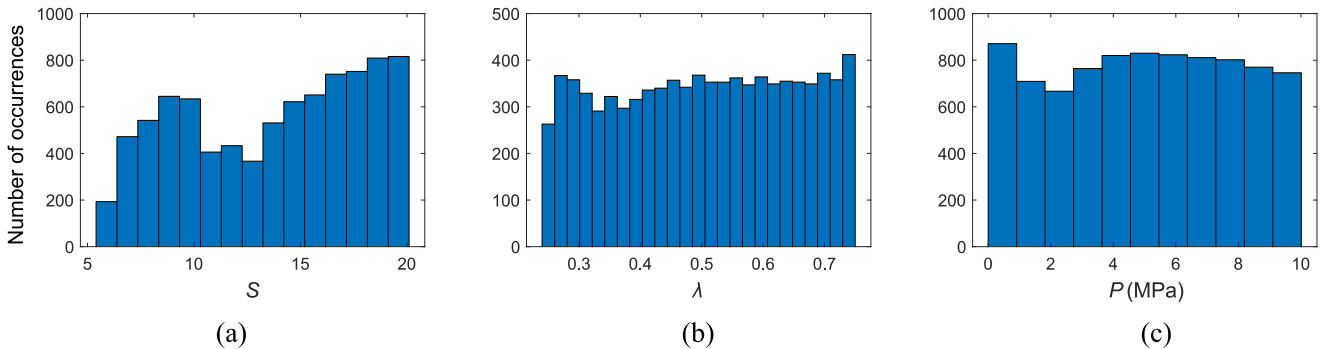


Figure 2: Distribution of isolator parameters: (a) shape factor, (b) slenderness ratio, and (c) bearing load.

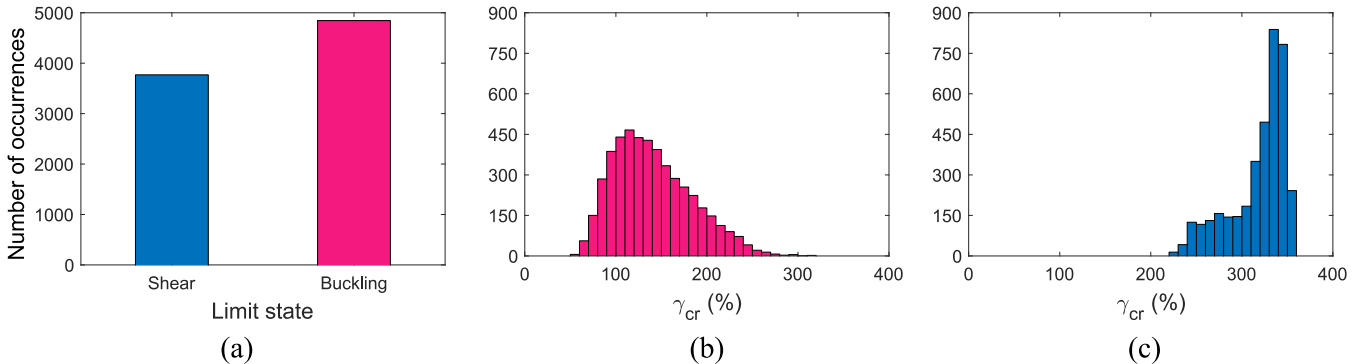


Figure 3: Distribution of limit states: (a) type and corresponding critical shear strain for (b) buckling and (c) shear failure.

Approximately 56% of the population of NR bridge isolator models failed under buckling, while the other 44% presented tearing of rubber characterizing shear failure (Figure 3a). Buckling LS occurs at lower shear strains, with mean of 140% and ranging from 55% to approximately 315% (Figure 3b). Isolators that are prone to shear failure present a greater capacity with mean shear strain of 320% and ranging from 220% to 360% (Figure 3c). Hence, an overlap of critical shear strains is observed between the two types of limit states.

STATISTICAL LEARNING USING GAUSSIAN PROCESS MODELS

Supervised machine learning comprises techniques that aim to code the relationship between a system's input (or covariates) \mathbf{x} and output (or responses) y . If the response is continuous, regression techniques are employed. Conversely, if the output is discrete (e.g., categories or classes), classification methods are used. Given the dual nature of the limit states of NR bridge isolators, a classification algorithm—to first define the domain of geometric and loading parameters within each limit state—followed by a regression algorithm—which approximates the corresponding critical shear strain—is deemed an appropriate framework to build a capacity model for NR seismic isolators.

Gaussian process can be employed to both regression and classification tasks. One of the main advantages of GP for statistical learning compared to more traditional approaches is that it is based on a nonparametric formulation in which the encoded relationship relies exclusively on the observed data to predict unseen quantities. A Gaussian process expands the definition of a Gaussian distribution to infinite dimensions to describe the prior knowledge of a function over its covariate domain. This prior can be converted into a posterior over functions in the presence of observed data based on Bayes rule. Owing to the Bayesian formulation of GP learning, a dual-layer GP approach can quantify the degree of uncertainty throughout the process. Thus, the first layer of the proposed surrogate model separates the two types of limit state using GPC while also measuring the importance of each system covariate. Based on the selected covariates within each limit state, a GP regression model estimates the distribution of critical shear strain of the elastomeric isolator. The formulation of Gaussian process for regression is briefly presented first. Its adaptation for classification purposes is shown next. These formulations are taken from Ref. [12-14].

Gaussian process regression

A Gaussian process expands the definition of a Gaussian distribution to infinite dimensions to describe the prior knowledge of a function over its covariate domain. This prior can be converted into a posterior over functions in the presence of observed data. Given a finite set of N data points $\mathbf{x} = \{\mathbf{x}_1, \dots, \mathbf{x}_N\}$, a GP assumes that the probability over the functions $y = f(\mathbf{x})$ is jointly Gaussian, i.e.:

$$f \sim \text{GP}(\boldsymbol{\mu}_G(\mathbf{x}), \boldsymbol{\Sigma}_G(\mathbf{x})) \quad (1)$$

where $\boldsymbol{\mu}(\mathbf{x})$ and $\boldsymbol{\Sigma}(\mathbf{x})$ denote the prior mean vector and the covariance matrix over \mathbf{x} . The covariance matrix is built upon a positive definite kernel function so that $\Sigma_{ij} = \sigma_G^2 \rho(\mathbf{x}_i, \mathbf{x}_j)$, where σ_G^2 is the overall covariance of random functions, and $\rho(\mathbf{x}_i, \mathbf{x}_j)$ is the correlation function that relates $f(\mathbf{x}_i)$ to $f(\mathbf{x}_j)$. A simple and commonly adopted kernel function is the squared-exponential (SE) correlation. In the case of multiple covariates, the SE correlation function with automatic relevance determination (ARD) is defined as:

$$\rho(\mathbf{x}_i, \mathbf{x}_j) = \prod_{k=1}^n \exp\left(-\frac{([\mathbf{x}_i]_k - [\mathbf{x}_j]_k)^2}{2\ell_k^2}\right) \quad (2)$$

where ℓ_k is the length-scale parameter for each covariate. The relevance of the covariate is measure by its length-scale parameter with respect to the training range. Further details on ARD are presented in the discussion of fitted models.

Considering a set of observed system inputs $D_x = \{\mathbf{x}_1, \dots, \mathbf{x}_D\}$ and outputs $D_y = \{f(\mathbf{x}_1), \dots, f(\mathbf{x}_D)\}$, the prior GP can be updated so that posterior predictions conditioned on the observation set $D = \{D_x, D_y\}$ can be made on unobserved covariates \mathbf{x}^* . The hyperparameters of the GP model $\boldsymbol{\theta} = [\sigma_G \ell_1 \dots \ell_k]$ must be learned from the observed data beforehand following Bayes rule and maximizing the likelihood $L(D_y | D_x, \boldsymbol{\theta})$. Once the model is trained, the posterior mean and covariance on unobserved covariates are assessed as:

$$\boldsymbol{\mu}_{*|D} = \boldsymbol{\mu}_* + \boldsymbol{\Sigma}_{G*}^T \boldsymbol{\Sigma}_G^{-1} (\mathbf{f} - \boldsymbol{\mu}_G) \quad (3)$$

$$\boldsymbol{\Sigma}_{*|D} = \boldsymbol{\Sigma}_* - \boldsymbol{\Sigma}_{G*}^T \boldsymbol{\Sigma}_G^{-1} \boldsymbol{\Sigma}_{G*} \quad (4)$$

where $\boldsymbol{\mu}_*$ and $\boldsymbol{\Sigma}_*$ are the prior mean and covariance on \mathbf{x}^* , and $\boldsymbol{\Sigma}_{G*}$ is the covariance between training (observed) and prediction covariates.

Gaussian process classification

Gaussian process classification (GPC) broadens GPR to classification problems, in which the response of the system is discrete (i.e., a class). More precisely, considering a problem with only two classes, GPC establishes the relationship between the continuous system input \mathbf{X} and a discrete output $y \in \{-1, +1\}$. By adopting the probit transformation $\Phi(\cdot)$ (i.e., the standard normal cumulative distribution function), the output of $f(\mathbf{x})$ of the GP model is mapped into the interval (0,1) that describes the conditional probability of $\mathbf{X} = \mathbf{x}$ corresponding to a class (i.e., $\Pr(Y = +1|\mathbf{X} = \mathbf{x})$). It is, therefore, a discriminative approach for classification, which means a conditional probability distribution is directly modelled at first so an optimal decision can be subsequently made to which class $\mathbf{X} = \mathbf{x}$ belongs. Besides, given that $f(\mathbf{x})$ is not directly observed (i.e., only the label $Y = +1$ or -1 is available), the mean and covariance for latent variables must be inferred for each covariate \mathbf{x} .

RESULTS AND DISCUSSION

The Gaussian process for machine learning (GPML) Matlab toolbox [12,15] is employed in the training and testing of the dual-layer GP models. Model predictability is measured using 5-fold cross-validation for both classification and regression steps. For the GPC step, confusion matrix metrics are used: accuracy and F-scores for each class. While accuracy is a global performance metric of classification models, the F-scores are better suited to indicate the balanced performance between classes [16]. For the GPR step, goodness-of-fit is measured using root mean squared error (RSME) and the coefficient of determination R^2 . Several covariance functions were investigated, and all presented similar performance. The comparison, therefore, is omitted for brevity. To improve the performance of the GP models, standardized covariates $\mathbf{z}_i = (\mathbf{x}_i - m_{x_i}) / s_{x_i}$ were used to uniformize the range of the investigated covariates, where m_{x_i} and s_{x_i} are the sample mean and standard deviation. In the classification phase, standardization of the input is made with respect to the entire dataset. In the regression phase, however, standardizations are made within each class.

Classification step

In the classification step, buckling is defined as $Y = +1$, while shear failure was defined as $Y = -1$. Decision boundary is set to $\Pr(Y = +1|\mathbf{X} = \mathbf{x}) = 0.5$, meaning that if the probability is greater than 0.5, the data point corresponds to the class $Y = +1$ (buckling limit state). Otherwise, the data point corresponds to the class $Y = -1$ (shear failure LS). The importance of each covariate is first assessed by training the model using all the covariates and then comparing the length-scale of each covariate ℓ_i to the sample standard deviation s_{x_i} . If the length-scale of a covariate is greater than two times the sample standard deviation, one can infer that the influence of the covariance on the system output is limited [12,13]. The length-scale parameters for the shape factor, slenderness ratio, and bearing load are, respectively, $\ell_{\text{classification}} = \{1.576, 0.537, 1.214\}$. Because the covariates are standardized, sample standard deviations are $s_{x_i} \approx 1$ for all the covariates. These length-scale parameters suggest that slenderness ratio has the greatest influence in determining if an isolator will fail by buckling or tearing by shear failure, followed by bearing load and shape factor with apparent comparable relevance.

The contour plots of the probability of a data point corresponding to the buckling limit state, i.e., $\Pr(Y = +1|\mathbf{X} = \mathbf{x})$ evidence the largest importance of slenderness ratio and bearing load in separating the two failure modes (Figure 4). For compressive loads greater than 5 MPa, the slenderness ratio varies within a narrow interval (between 0.35 and 0.4). This reinforces the suggested threshold $\lambda_{lim} = 0.4$ to separate slender from non-slender isolators [4-6]. Under lower bearing loads ($P < 5$ MPa), however, slender isolators (slenderness ratios between 0.4 and 0.7) may also undergo shear failure. Moreover, buckling is not likely to occur for compressive loads below 2 MPa even for slender isolators. Additionally, the contour plots with respect to λ and P indicate the negligible influence of the shape factor in separating the two LS: the decision boundary remains practically constant while the shape factor is varied from 6 to 20. Similar patterns of the contour plots are observed when the covariates vary within the investigated intervals. While contour plots with respect to the shape factors varying from 6 to 20 show a curved decision boundary, contour plots with respect to slenderness ratio and bearing load depict an approximately straight decision boundary that moves downwards while the values of P or λ are increased, respectively.

To further investigate the importance of each parameter, classification is performed with partial covariate sets (Table 1). Using only the shape factor resulted in a GPC model that classifies all the data points as buckling. This is evidenced by the accuracy being equal to the proportion of numerical models that failed by buckling in the dataset, and the F-score of the shear failure class was not calculated because false negative and true negative cases are all zero. The other one-covariate sets (i.e., containing only either slenderness ratio or bearing load) performed fairly with respect to the model accuracy. However, the F-scores indicate the unbalanced classification between the two classes. The same is observed for the two-covariate sets containing the shape factor. Finally, the covariate set comprised by slenderness ratio and bearing load has a comparable performance to the GPC model built upon the entire covariate set, suggesting that shape factor has a negligible influence in separating the two types of limits states in this population of natural rubber bridge isolators.

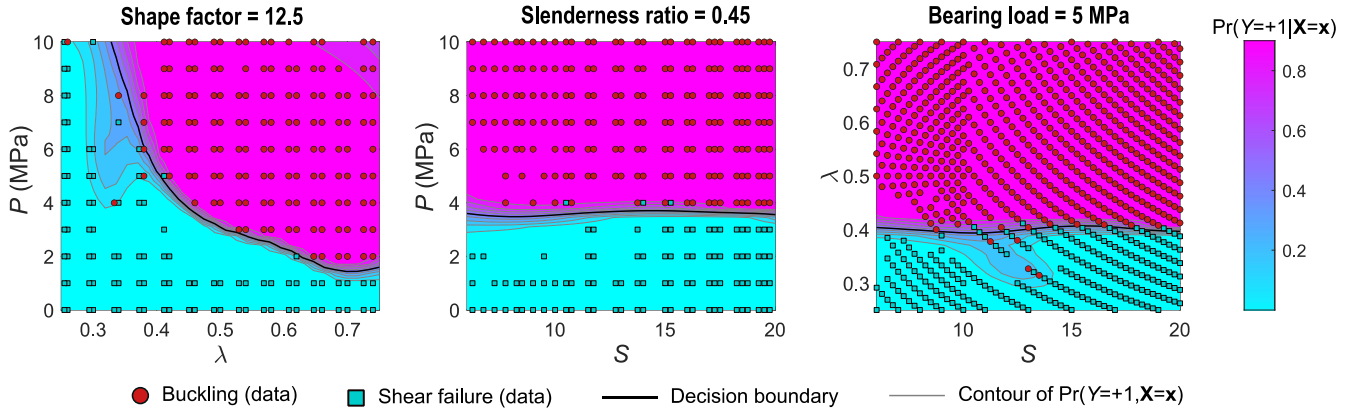

 Figure 4: Contour plots of $Pr(Y = +1|X = \mathbf{x})$ with respect to shape factor, slenderness ratio, and bearing load.

Table 1: 5-fold cross-validation scores for the GPC step using different covariate sets.

$\mathbf{X} =$	Accuracy	F-score (buckling)	F-score (shear failure)
$\{S\}$	0.567	0.723	n.a.
$\{\lambda\}$	0.810	0.852	0.739
$\{P\}$	0.811	0.833	0.676
$\{S, \lambda\}$	0.806	0.844	0.742
$\{S, P\}$	0.788	0.835	0.703
$\{\lambda, P\}$	0.988	0.989	0.986
$\{S, \lambda, P\}$	0.992	0.993	0.991

Regression step

After classifying the data points as buckling or shear failure, regression is performed within each limit state to estimate the critical shear strain based on the provided covariates. Because ultimate shear strain is a positive value, a logarithmic transformation is applied so $Y_{reg} = \ln \gamma_{cr}$. Also, system response is assumed error free since it was generated from a numerical model. Based on the results of the classification step, only the two covariate sets that best performed are chosen to assess the relevance of the covariates in approximating the shear strain capacity of the rubber isolators: $\mathbf{X}_1 = \{S, \lambda, P\}$ and $\mathbf{X}_2 = \{\lambda, P\}$. Moreover, regression is also performed on the entire dataset without classification (i.e., combined buckling and shear failure data points) for comparison with the dual-layer approach. The prior mean is assumed as zero ($\boldsymbol{\mu}_G = \mathbf{0}$) in Eq. (1), which is a frequent approach given that the covariance function relates one observation to another [17]. The fitted hyperparameters are again used to study the relevance of each covariate (Table 2), this time in estimating the critical shear strain of the NR isolator. Shape factor seems less relevant in approximating the capacity of isolators prone to buckling compared to slenderness and compressive load with similar importance. On the other hand, shape factor comes as the most important parameter when estimating the critical shear strain of isolators prone to shear. If the shape factor is omitted from the training of the regression model, the variability of the fitted model increases, particularly for the buckling LS.

Table 2: Hyperparameters of the Gaussian process regression models.

Covariate set	Limit state	Length-scale			Standard deviation (σ_G)
		Shape factor (ℓ_S)	Slenderness ratio (ℓ_λ)	Bearing load (ℓ_P)	
$\mathbf{X}_1 = \{S, \lambda, P\}$	Buckling	3.344	1.123	1.254	1.639
	Shear	0.585	0.776	0.923	1.502
	Buckling/Shear	1.692	0.342	0.460	1.361
$\mathbf{X}_2 = \{\lambda, P\}$	Buckling	–	7.477	2.981	2.654
	Shear	–	3.519	2.131	1.862
	Buckling/Shear	–	0.766	0.486	1.541

The scatter plots of the observed against predicted values of γ_{cr} are used to depict the performance of each model along with the regression metrics RMSE and R^2 (Figure 5). For the entire covariate set, the coefficients of determination are comparable with or without previous classification. The RMSE values, however, indicate that the GPR models perform better when the

limit states are separated beforehand. Accordingly, significant improvement is particularly achieved for isolators subjected to buckling limit state. With respect to the importance of the covariates, removing the shape factor from the covariate set has a moderate impact on the regression model performance. The larger dispersion of the estimated ultimate shear strain observed in the scatter plots is confirmed by the RMSE values that are at least three times larger than when the entire covariate set is used for training the GPR model. Moreover, contrarily to the improvement provided by the classification when the shape factor is considered, the performance of the GPR model trained without classification on the partial covariate set is fairly similar to the separated limit states.

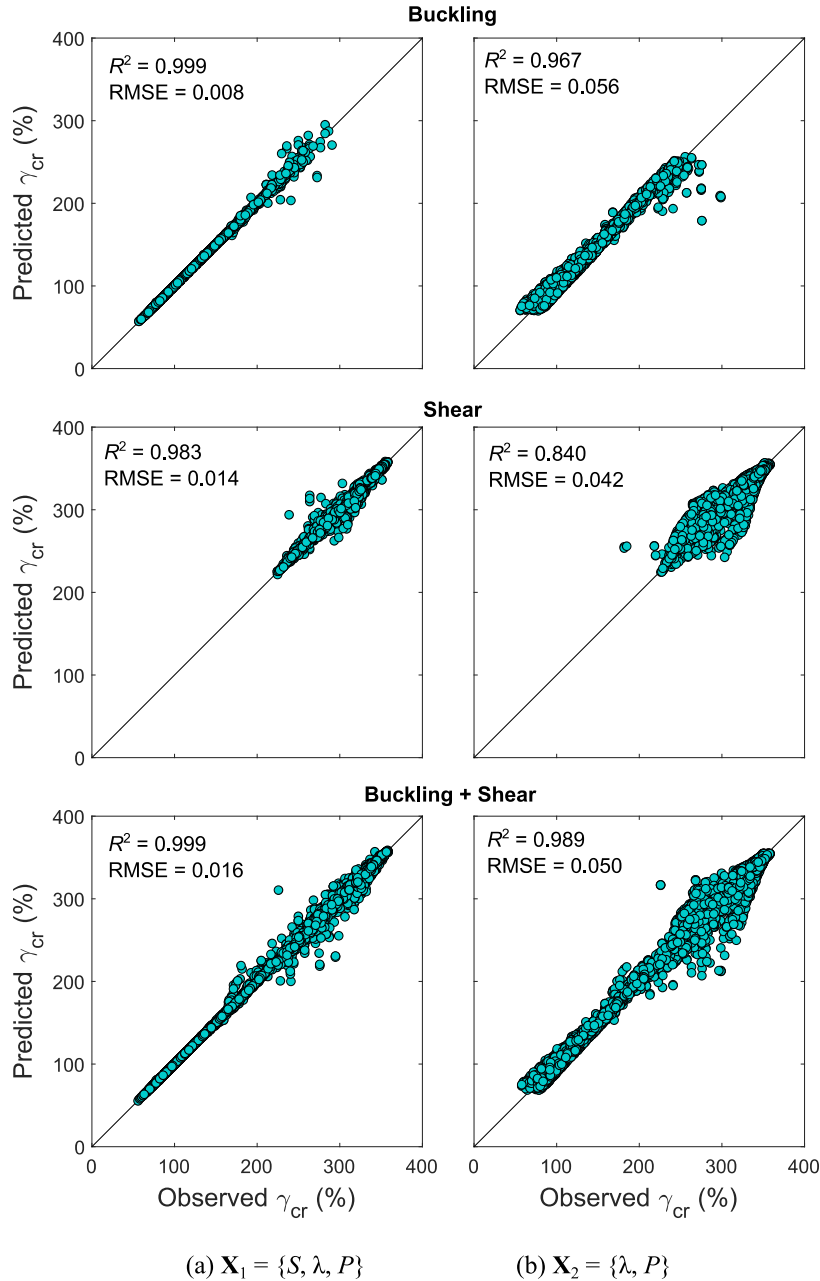


Figure 5: Observed versus predicted critical shear strains from GPR for: (a) entire and (b) partial covariate sets.

Fragility models

Based on Equations (3) and (4), the posterior mean and the variance of the distribution of critical shear strains can be predicted for a set of system parameters. These values can, therefore, be used in the construction of fragility functions for NR bridge isolators. Given that the critical shear strains were transformed into the lognormal space, the fragility functions follow a

lognormal distribution with the parameters being estimated by the GP model for buckling and shear failure. One advantage of Gaussian process regression compared to more typical regression techniques (e.g., linear regression) is its capacity to model the uncertainty in extrapolation [13]. Fragility curves were built for both limit states considering a variation of slenderness ratios within and outside the ranges used for training the surrogate model, while shape factor was set to 12.5 and bearing load to 5 MPa (Figure 6). For both limit states, the isolator capacity decreases for increasing slenderness ratios within the training interval (λ between 0.25 and 0.75—Figure 2b). Also, the respective fragility functions show low uncertainty with fragility curves that are like step functions. In the case of isolators prone to buckling (Figure 6a), for slenderness ratios greater than 0.75, the shear strain capacity still decreases as λ is incremented, while the dispersion increases as the isolators becomes slenderer. In the case of isolators prone to shear failure (Figure 6b), for $\lambda < 0.25$ the dispersion is also verified as expected. The expected capacity of the isolator to deform in shear, however, decreases as λ is reduced, which seems contradictory to the observed trend. This may be explained by the assumption of the prior mean of the GPR model being equal to zero and the fitted length-scale for slenderness (Table 2). Extrapolated posterior mean rapidly decreases to zero as one uses slenderness ratios that are far from the limits of covariate values used to build the GP regression model.

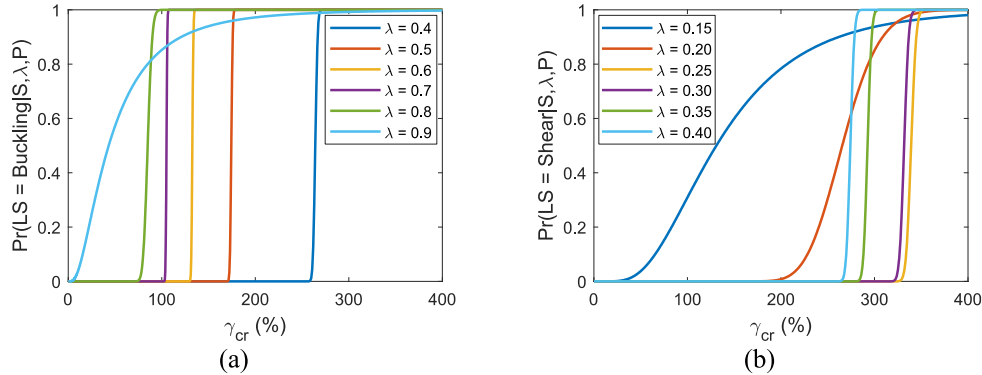


Figure 6: Fragility curves of NR bridge isolators with varying slenderness ratios for: (a) buckling, and (b) shear failure limit states.

CONCLUSIONS

A dual-layer Gaussian process surrogate model is proposed to define the limit state of natural rubber bridge isolators based on shape factor, slenderness ratio, and bearing load. The GP surrogate model can efficiently separate the two types of limit states (buckling and shear failure) and approximate the corresponding critical shear strain. The combined influence of the isolator geometric and loading parameters suggests that a single threshold of slenderness ratio may only be adequate for more heavily loaded isolators. For isolators subjected to lower compressive loads, a combination of slenderness ratio and bearing load can more efficiently separate the two types of limit states. The shape factor has a negligible role in the definition of the type of failure. Completely ignoring the shape factor, however, significantly increases the error in approximating the shear strain capacity of isolators prone to both shear failure and buckling. The probabilistic formulation used to build the surrogated models is also leveraged for the construction of fragility curves, which are of main interest in the application of PBEE. Given the posterior mean and variance of the regression step, fragility curves are readily constructed to assess the shear strain capacity of natura rubber bridge isolators. A potential limitation of the assumptions is observed when fragilities are extrapolated. Using a semi-parametric approach to GP learning using basis functions could overcome this limitation. Other features of the training and modelling process should also be further investigated, such as the influence of the distribution of the covariates. Future work is sought in this direction along with the development of design charts and fragility curves considering the variability of isolator properties.

ACKNOWLEDGMENTS

The authors gratefully acknowledge the Ministère des Transports du Québec and Mitacs (grant number IT23417) for their financial support of this project, and Olivier Gauron, Adamou Saidou, and Arnaud Busson for the database used in this study.

REFERENCES

- [1] Padgett, J. E. and DesRoches, R. 2008. Methodology for the development of analytical fragility curves for retrofitted bridges. *Earthquake Engineering & Structural Dynamics*, **37**(8): 1157-1174.
- [2] Siqueira, G. H., Sanda, A. S., Paultre, P., and Padgett, J. E. 2014. Fragility curves for isolated bridges in eastern Canada using experimental results. *Engineering Structures*, **74**: 311-324.

- [3] Bandini, P.A.C, Padgett, J.E., Paultre, P., and Siqueira, G.H. 2022. Seismic fragility of bridges: An approach coupling multiple-stripe analysis and Gaussian mixture for multicomponent structures. *Earthquake Spectra*; **38**(1): 254–282.
- [4] Gauron, O., Saidou, A., Busson, A., Siqueira, G.H., Paultre, P. 2018. Experimental determination of the lateral stability and shear failure limit states of bridge rubber bearings, *Engineering Structures* **174**: 38–48.
- [5] Montuori, G. M. Mele, E. Marrazzo, G. Brandonisio, G. De Luca, A. 2016. Stability issues and pressure-shear interaction in elastomeric bearings: the primary role of the secondary shape factor, *Bulletin of Earthquake Engineering* **14**: 569–597
- [6] Bandini, P. A. C., Gauron, O., Saidou, A., Busson, A., Paultre, P. Probabilistic lateral stability and shear failure limit states of bridge natural rubber bearings. *Engineering Structures*, 289: 116257.
- [7] Saidou, A., Gauron, O., Busson, A., Paultre, P. 2021. High-order finite element model of bridge rubber bearings for the prediction of buckling and shear failure, *Engineering Structures* **240**: 112314.
- [8] Priestley, M. Calvi, G. 1996. *Seismic design and retrofit of bridges*, John Wiley and Sons, New York.
- [9] Nagarajaiah, S. Ferrell, K. 1999. Stability of elastomeric seismic isolation bearings, *Journal of Structural Engineering*. **125** (9): 946–954.
- [10] Weisman, J. Warn, G. 2012. Stability of elastomeric and lead-rubber seismic isolation bearings, *Journal of Structural Engineering*. **138** (2): 215–223.
- [11] Siqueira, G. H. Tavares, D. H. Paultre, P. Padgett, J. E. 2014 Performance evaluation of natural rubber seismic isolators as a retrofit measure for typical multi-span concrete bridges in eastern Canada, *Engineering Structures* **74**: 300–310.
- [12] Rasmussen, C. E. and Williams, C. K. I. 2006. *Gaussian Processes for Machine Learning*. The MIT Press, Cambridge, Massachusetts.
- [13] Goulet, J.-A. 2020. *Probabilistic Machine Learning for Civil Engineers*. The MIT Press, Cambridge, Massachusetts.
- [14] Murphy, K. P. 2012. *Machine Learning – A Probabilistic Perspective*. The MIT Press, Cambridge, Massachusetts.
- [15] Rasmussen, C. E. and Nickisch, H. 2022. *The GPML Toolbox version 4.2*.
- [16] Kiani, J. Camp, C., Pezeshk, S. 2019. On the application of machine learning techniques to derive seismic fragility curves. *Computers and Structures* **218**: 108–122.
- [17] Ebdem, M. 2015. Gaussian processes: A quick introduction. *arXiv preprint (1505.02965) [math.ST]*.